Surface Modifications

Deutsche Ausgabe: DOI: 10.1002/ange.201600080
Internationale Ausgabe: DOI: 10.1002/anie.201600080

Bio-Inspired Renewable Surface-Initiated Polymerization from Permanently Embedded Initiators

*Tao Du, Bin Li, Xiaolong Wang, Bo Yu, Xiaowei Pei, Wilhelm T. S. Huck, and Feng Zhou**

Abstract: *Herein, we describe a simple and robust approach to repeatedly modify surfaces with polymer brushes through surface-initiated atomic transfer radical polymerization (SI-ATRP), based on an initiator-embedded polystyrene sheet that does not rely on specific surface chemistries for initiator immobilization. The surface-grafted polymer brushes can be wiped away to expose fresh underlying initiator that re-initiates polymerization. This strategy provides a facile route for modification of molded or embossed surfaces, with possible applications in the preparation of fluidic devices and polymer-embedded circuits.*

Surface modifications with organic molecules afford good control over the surface and interfacial properties of a material irrespective of its bulk property, and therefore have found widespread applications in antifouling,[1] electronic devices,[2] stimuli-responsive systems,[3] and biosensing.[4] A number of strategies have been developed for modifications either through physisorption or chemical bond formation, such as self-assembled monolayer (SAM) formation,[5] Langmuir–Blodgett deposition,[6] layer-by-layer assembly,[7] and the grafting to or grafting from techniques to form covalently attached polymer films.[8] By adopting different anchoring chemistries, an impressive range of inorganic and organic substrates can be modified.[9] The grafting from approach, in particular, which uses surface-initiated controlled radical polymerizations,[10] has long been used as an essential tool for tailoring surface properties, as it shows excellent tolerance to functional groups and impurities,[11] and is suitable for a variety of polymerizable monomers.[12] Among them, surface-initiated atom transfer radical polymerization (SI-ATRP) has been extensively used for surface modification to prepare highly tailored thin films in which chemical composition, thickness, and architecture were precisely controlled.[13] However, to date, all of these synthetic routes are based on single-use substrates.[14] Ma et al. have used an initiator embedded polydimethylsiloxane (PDMS) to carry out SI-ATRP, but never tried the second polymerization modification.[15] Recently, Du Prez et al. reported a "print, erase, and reprint" approach to rewritable polymer brush micropatterns on glass and silicon substrates based on click chemistry.[16] Herein, we report a facile method for grafting polymer layers on the initiator permanently embedded polymeric substrate so that substrate can re-initiate polymerization when the grafted polymer layer is wiped away.

As shown in Scheme 1, a methacrylate monomer pendant with an ATRP initiator moiety was copolymerized with styrene monomer through the free radical bulk polymerization process to give the ATRP initiator embedded polystyrene (iePS). Initiator-embedded substrate is akin to soil with living seeds underneath, and the polymerization will be re-initiated when the initiators contact with monomers (Supporting Information, Movie S1). For instance, mechanically polishing the surface will regenerate the active bromine initiator for the next polymer grafting, which can be carried on many times (Scheme 1; Supporting Information, Movie S2).

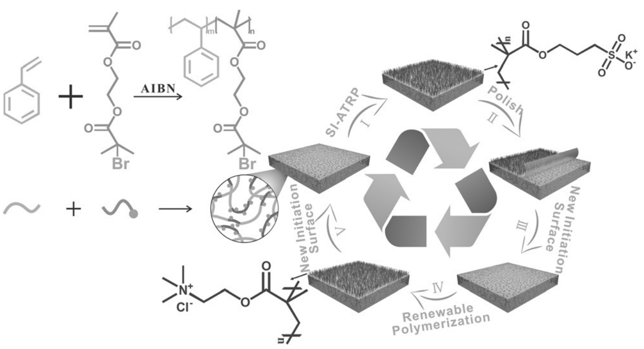

Scheme 1. Diagram of the synthesis of initiator-embedded polystyrene (iePS) substrates and subsequent renewable grafting polymerization. Polymer layers grafted from iePS can be mechanically wiped away, exposing the underlying initiator moiety again for grafting polymerization repeatedly.

Typically, a 5 wt% solution of 2-(2-bromoisobutyryloxy) ethyl methacrylate (BrMA) as a co-monomer was added to the styrene monomer (a crosslinker may or may not be required), in the presence of a small amount of azobisisobutylnitrile (AIBN) as the radical initiator. This mixture was heated up to 80 °C for a few minutes to obtain a prepolymer that was then cooled and poured into a glass petri dish. The

---

[*] T. Du, Dr. B. Li, Prof. X. Wang, Dr. B. Yu, Prof. X. Pei, Prof. F. Zhou
State Key Laboratory of Solid Lubrication
Lanzhou Institute of Chemical Physics
Chinese Academy of Sciences
Lanzhou, 730000 (China)
E-mail: zhouf@licp.cas.cn

Prof. W. T. S. Huck
Institute for Molecules and Materials
Radboud University
Heyendaalseweg 135, 6525 AJ Nijmegen (The Netherlands)

T. Du
University of Chinese Academy of Sciences
Beijing, 100049 (China)

Supporting information, including experimental details and data, for this article can be found under http://dx.doi.org/10.1002/anie.201600080.

polymerization was carried out at 80 °C for 24 h and at 120 °C for another 24 h under a nitrogen atmosphere. After polymerization, the iePS sheet was detached from the petri dish and extracted thoroughly with excess methanol in a Schlenck tube to remove unreacted styrene monomers and AIBN initiator. The characterization of the iePS is given in the Supporting Information (Figures S3–S6), verifying the successful incorporation of initiator.

The key factor in successfully implementing SI-ATRP is that the active Br atoms are exposed at the surface. X-ray photoelectron spectroscopy (XPS) was used to investigate the chemical compositions of the surface, as well as the in-depth element profile by in situ etching the iePS substrate with argon ion. Compared with the pure PS, the appearance of Br 3d peak at 70 eV indicates the existence of ATRP initiator on the surface of iePS (Figure 1 a). The surface atom percentages of C and O are 94.89 % and 4.44 %, while Br has an atomic content of 0.67 %. Figure 1 b illustrates the XPS depth profile of the iePS sample with the etching time at a speed of 5 nm min^{-1}. It was seen that the atom percentage of Br increases slightly from 0.61 % to 1.4 %, and levels off after 60 s of etching. The atom percentage of C increases from 94.95 % to 97.32 %, whereas the atom percentage of O decreases from 4.44 to 1.28 %. The ^{1}H NMR spectrum was also obtained to identify the content of BrMA in iePS structure. The data is given in Figure S3, and the calculated molar ratio of BrMA is 0.0231, which is in agreement with the feeding molar ratio. The cross section of the iePS sheet was also analyzed by scanning electron microscopy (SEM) and energy dispersive X-ray spectroscopy (EDX), which revealed that the C, O, and Br are uniformly distributed deep into the bulk material (Figure 1 d).

The SI-ATRP of several representative monomers were carried from a single iePS substrate. The surface elements of the substrate after each step of the polymerization process were examined by XPS (Figure 1 a). First, anionic poly 3-sulfopropyl methacrylate potassium salt (PSPMA) was grafted on the flat iePS surface (blue curve), the characteristic S 2p peak at 168 eV and K 2p peak at 293 eV clearly demonstrated the successful polymerization of SPMA. After mechanically polishing the PSPMA layer by using an abrasive paper (180-grit, silicon carbide), the Br atoms appeared on the surface, as indicated by the Br 3d peak at 70 eV, and the density of the O 1s peak at 532 eV was significantly reduced. Then the cationic poly 2-(methacryloyloxy)ethyl-trimethylammonium chloride (PMETAC) was grafted, as indicated by the Cl 2p peak at 198 eV and N 1s peak at 402 eV. Other polymers, anionic poly sodium methacrylate (PMAA-Na) and cationic poly 2-(dimethylamino)ethyl methacrylate (PDMAEMA), zwitterionic poly [2-(methacryloyloxy)ethyl]-dimethyl(3-sulfopropyl)ammonium hydroxide (PSBMA), neutral poly 2-hydroxyethyl methacrylate (PHEMA), and poly *N*-isopropyl acrylamide (PNIPAm) were grafted on the iePS substrate sequentially by repeating the above procedures to verify that this permanent initiator-embedded PS substrate is able to initiate ATRP with various types of polymers. All of these polymerizations could be carried out in aqueous solvents that do not solvate the iePS substrate. The preserved chain end functionality was demonstrated by the presence of the Br 3d peak in the survey scan of the respective polymer layers. This may offer the possibility of preparing copolymer layers through further SI-ATRP.

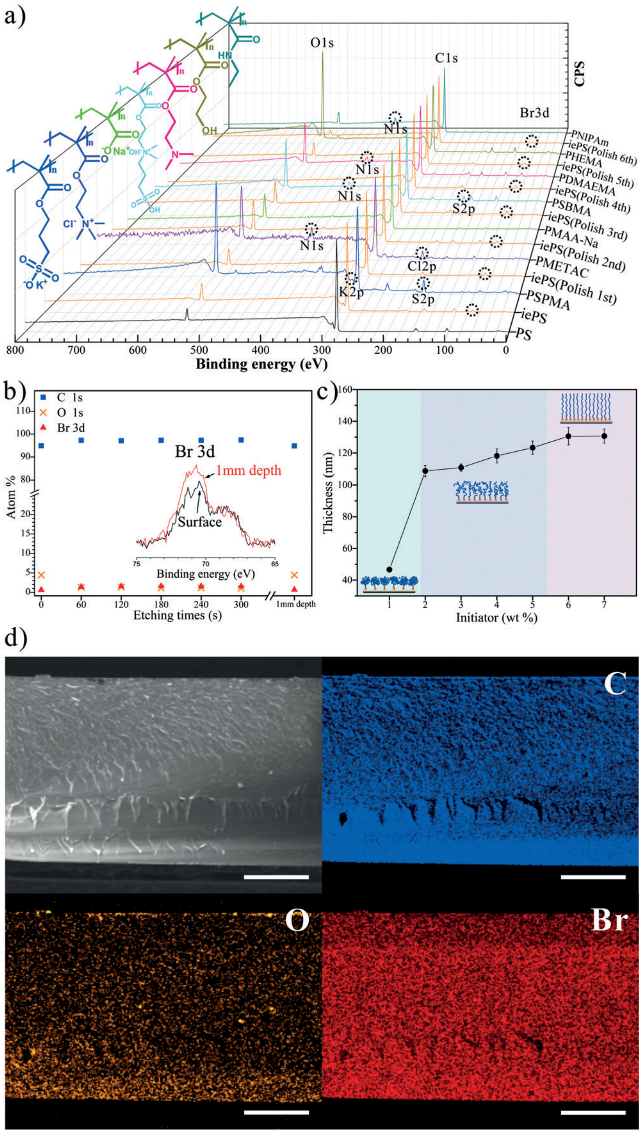

Figure 1. a) XPS confirmed successful surface modification from iePS through renewable SI-ATRP of seven representative monomers. All of the spectra were aligned to the C 1s peak. b) XPS depth profile of iePS by argon ion etching. The 1 mm depth surface was cut manually, not by etching. The inset is the high resolution XPS of Br 3d of the outermost surface and 1 mm depth surface. c) PSPMA brush thickness as a function of weight percentage content of BrMA initiator. Lines were added to guide the eyes. d) SEM cross-sectional image of the iePS with its corresponding EDX mapping indicating carbon (blue), oxygen (yellow), and bromine (red). Scale bars = 25 μm.

The content of BrMA initiator in iePS dictates the density of grafted polymer chains. Although the actual density is hard to measure, we have used the dry thickness obtained under the same experiment conditions to indicate the grafting density (the grafted polymers are supposed to have similar molecular weights at the same polymerization time). As shown in Figure 1 c, at the polymerization time 60 min, the PSPMA dry thickness was 47 nm at 1 wt % of BrMA initiator, dramatically increased to 109 nm when the content was up to 2 %, and thereafter it increased with increasing the content of the BrMA initiator until it reached a constant value at about 130 nm at 6 % content. This may indicate that polymer chains evolve from a mushroom conformation to more stretched conformations when the initiator density was increased.[17]

The grafting methodology allows us to change the surface physiochemical properties on one substrate by changing the surface chemistries. Figure S7 shows that different polymers were successively grafted on a flat iePS and displayed different water contact angles. After being polished with abrasive paper, the surface became rougher and more hydrophilic or more hydrophobic when grafting the same polymers. Figures S8 and S9 show the cytocompatibility and algae adhesion on the surface decorated with polymer layers. All of these properties have been extensively researched and will not be dwelled on here.

We were more interested in the recovery of the lubricating properties of a surface when it is worn. Polyelectrolyte brushes are able to reduce friction coefficients owing to the high hydration of charged fragments on the polymer chains and the exceptional resistance to mutual interpenetration displayed by the compressed yet swollen brushes in aqueous environments.[18] PSPMA-decorated flat iePS substrate has a very low coefficient of friction (COF) of about 0.2 (Figure 2), then the COF increased to approximately 2.8 when the PSPMA layer was mechanically removed by an abrasive paper and washed ultrasonically (Figure 2). The iePS surface was re-initiated to graft the PSPMA and then removed mechanically. The friction behavior is almost reversible: the COF can be switched repeatedly and reproducibly. This renewable friction tests showed the PSPMA-decorated iePS substrates have a good lubricating behavior. These findings have important implications for artificial implant design and biolubrication.

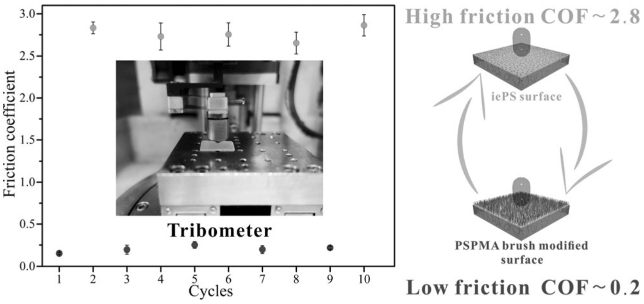

Figure 2. Reversible switch of coefficient of friction on a sample surface between low friction ($\mu \approx 0.2$) upon PSPMA decoration and high friction ($\mu > 2$) when polymer was wiped away. (load 0.1 N, velocity 0.001 m s^{-1}, reciprocating amplitude 5 mm). The inset is the tribometer UMT-2.

The extraordinary feature of the surface modification methodology is to make robust patterns that are not floating on substrate surface (such as those prepared with microcontact printing + SIP),[19] but embedded in the sublayer of the substrate, making these patterns scratch-resistant. To illustrate this, mechanical machining, hot embossing techniques, and laser surface texturing were used to fabricate patterns and derived reactions. The exemplified procedures are shown in Figure 3 a. The oxygen plasma was first used to break the C–Br bond to deactivate the surface.[20] Then the surface was carved to give a number of grooves that will expose initiator (yellow lines in Figure 3 a and the second photograph in Figure 3 b) so that the modification of PMETAC brushes only occurs in the grooves (the purple lines in Figure 3 a). Then the sample was immersed into $(NH_4)_2PdCl_4$ aqueous solution. $PdCl_4^{2-}$ moieties were immobilized onto the PMETAC through ion exchange and served as an effective catalyst for electroless plating (ELP) of Ni, Cu,

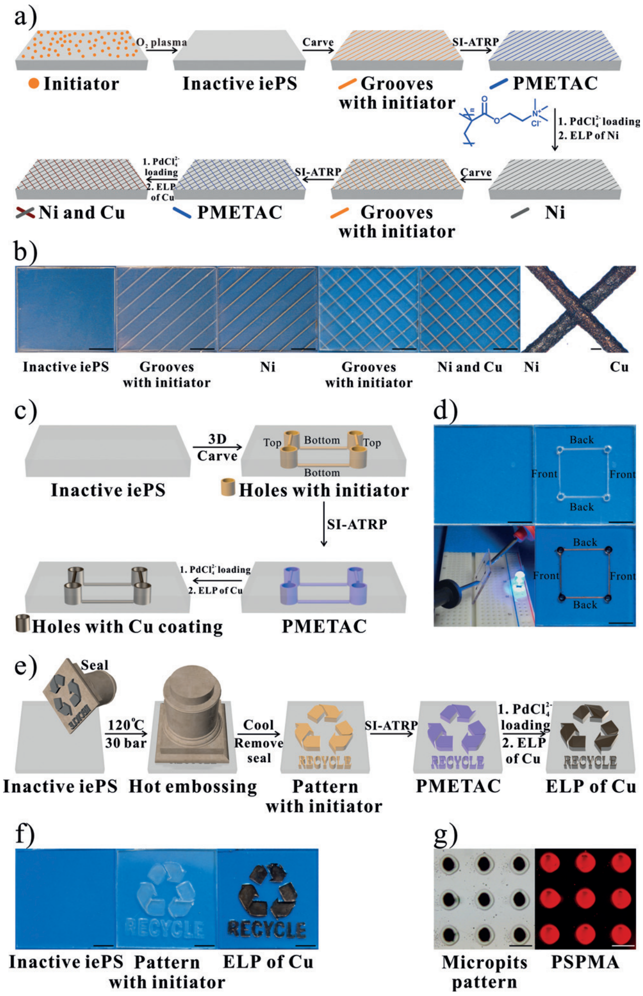

Figure 3. a) Diagram of the steps entailed in the renewable surface metallization by electroless plating of Ni and Cu. b) Photographs of the iePS sheet metallized with Ni and Cu stripes (scale bars, 5 mm), and the magnified picture of the intersection of two metals. Scale bars = 200 µm. c) Fabrication of stereoscopic Cu wires inside the iePS. d) Photograph of three-dimensional Cu circuit, illuminating a blue LED when the two metal probes between the two points on the different side are connected. Scale bars = 5 mm. e) Representation of surface metallization by hot embossing. f) Photograph of the hot embossed iePS sheet with concave pattern RECYCLE, and after ELP with Cu. Scale bars = 5 mm. g) The optical photographs of the laser micromachining fabricated micro-pits (diameter = 25 µm, depth = 5 µm) and fluorescence image of rhodamine 6G-stained PSPMA-grafted micropits. Scale bars = 50 µm.

and other metals.[21] The grooves with 200 μm width and 24 μm depth were finally coated with a layer of Ni by immersing into a laboratory-made Ni plating bath (black lines in Figure 3a and the third picture in Figure 3b). For the most prominent feature of this renewable SI-ATRP method, the process can be continuously implemented by repeating the above steps. As a proof-of-concept, a second set of carved grooves perpendicular to the above Ni stripes (the fourth photograph in Figure 3b) were manufactured for executing the ELP of Cu (crimson lines in Figure 3a). We ended up with the Ni- and Cu-striped wires embedded in the iePS substrate (the fifth and sixth photograph in Figure 3b). The feature sizes of the patterns could be further miniaturized by applying high-resolution micromachining techniques.[22]

In addition to sub-surface metallization, three-dimensional electroless plating of stereoscopic Cu conductive wires inside the iePS substrate can also be realized readily (Figure 3c and d). Four holes with a diameter of 1 mm were drilled in the vertical direction and each were connected with two grooves on the front side and two grooves on the back side in a horizontal direction. In this way, the three-dimensional Cu structure can be prepared. A simple circuit with a 3 V battery, which consists of one electrical contact of a blue LED and the three-dimensional Cu overcoatings structure, was bridged to test the electrical conductivity (Figure 3d; Supporting Information, Movie S3). When the metal probe contacted between the two points, whether on the same side or different side, the LED turned on immediately.

Hot embossing is a widely used stamping method to pattern a softened polymer by raising the temperature of the polymer just above its glass transition temperature. The goal of the present work is to demonstrate the possibility of combining hot embossing with the growth of polymer brushes. As shown in Figure 3e, hot embossing was carried out on a plasma-treatment-inactive iePS with a bronze seal with a convex "RECYCLE" pattern (Figure S10) heated to 120 °C. At this temperature above the glass transition temperature, the amorphous portions of the polymer softened, the chain segments rearranged in the embossed area, and the Br atoms are re-exposed on the surface. To confirm this assumption, XPS elemental analysis was performed to verify the presence of initiator on the stamped area (Figure S11). There were no Br 3d signals at 70 eV for the inactive surface (black in Figure S11). However, at the hot embossed area, the Br 3d peak at 70 eV appeared (yellow in Figure S11). The hot embossing area could indeed be modified with polymer layers, but not from the inactive area. Similarly, the hot embossing area could be successfully plated with Cu (Figure 3f).

The use of laser micromachining on polymer to fabricate patterns or channels has been widely used as a pivotal tool to construct microfluidic chips.[23] It is also compatible with the present approach to make patterned polymer brushes on this iePS substrate, with the prospect of some new applications of these patterns.[24] The micro-pits array (3 × 3), of approximately 25 μm diameter and 5 μm depth, were fabricated on the inactive iePS sheet by laser micromachining (Figure 3g). The burning of iePS on the shinning area will expose the embedded initiator on the edge. XPS elemental analysis showed that the micro-pits had the Br 3d peak at 70 eV (red in Figure S11). The anionic PSPMA polymer brushes were subsequently grafted and stained by cationic rhodamine-6G. In the fluorescence image in Figure 3g, the red fluorescence color around the micro-pits array confirms successful PSPMA grafting. An attractive characteristic of laser micromachining is the possibility to fabricate complex patterns by readily construct miscellaneous patterns, even microfluidic channels, which, followed by surface grafting, allow fabrication of chemically modified micro-channels.

In conclusion, we have developed a renewable SI-ATRP method to graft various polymers continuously on an ATRP initiator-embedded polystyrene sheet. This new method has outpaced the traditional surface-grafting technologies owing to unlimited grafting cycles and its exquisite control over chemical composition, film architecture, and functionalities, which can be easily manipulated through straightforward preparative procedures. Interestingly, it can be combined with carving, micromachining, and hot embossing, and allows polymer grafting and metal deposition stereoselectively.

Acknowledgements

This work was financially supported by NSFC (21434009, 51573198).

Keywords: bio-inspiration · patterns · polymer brushes · renewable materials · surface-initiated polymerization

How to cite: *Angew. Chem. Int. Ed.* **2016**, *55*, 4260–4264
Angew. Chem. **2016**, *128*, 4332–4336

---

[1] J. A. Callow, M. E. Callow, *Nat. Commun.* **2011**, *2*, 244.
[2] F. Huo, Z. Zheng, G. Zheng, L. R. Giam, H. Zhang, C. A. Mirkin, *Science* **2008**, *321*, 1658–1660.
[3] M. A. C. Stuart, W. T. S. Huck, J. Genzer, M. Muller, C. Ober, M. Stamm, G. B. Sukhorukov, I. Szleifer, V. V. Tsukruk, M. Urban, F. Winnik, S. Zauscher, I. Luzinov, S. Minko, *Nat. Mater.* **2010**, *9*, 101–113.
[4] W. Senaratne, L. Andruzzi, C. K. Ober, *Biomacromolecules* **2005**, *6*, 2427–2448.
[5] A. Ulman, *Chem. Rev.* **1996**, *96*, 1533–1554.
[6] P. G. de Gennes, *Colloid Polym. Sci.* **1986**, *264*, 463–465.
[7] Y. Lvov, K. Ariga, I. Ichinose, T. Kunitake, *J. Am. Chem. Soc.* **1995**, *117*, 6117–6123.
[8] a) S. Minko, S. Patil, V. Datsyuk, F. Simon, K.-J. Eichhorn, M. Motornov, D. Usov, I. Tokarev, M. Stamm, *Langmuir* **2002**, *18*, 289–296; b) K. Matyjaszewski, H. Dong, W. Jakubowski, J. Pietrasik, A. Kusumo, *Langmuir* **2007**, *23*, 4528–4531.
[9] R. Barbey, L. Lavanant, D. Paripovic, N. Schüwer, C. Sugnaux, S. Tugulu, H.-A. Klok, *Chem. Rev.* **2009**, *109*, 5437–5527.
[10] S. Edmondson, V. L. Osborne, W. T. S. Huck, *Chem. Soc. Rev.* **2004**, *33*, 14–22.
[11] a) A. de los Santos Pereira, N. Y. Kostina, M. Bruns, C. Rodriguez-Emmenegger, C. Barner-Kowollik, *Langmuir* **2015**, *31*, 5899–5907; b) A. F. Hirschbiel, S. Geyer, B. Yameen, A. Welle, P. Nikolov, S. Giselbrecht, S. Scholpp, G. Delaittre, C. Barner-Kowollik, *Adv. Mater.* **2015**, *27*, 2621–2626.
[12] S. Banerjee, T. K. Paira, T. K. Mandal, *Polym. Chem.* **2014**, *5*, 4153–4167.
[13] a) J. E. Poelma, B. P. Fors, G. F. Meyers, J. W. Kramer, C. J. Hawker, *Angew. Chem. Int. Ed.* **2013**, *52*, 6844–6848; *Angew.*

Chem. **2013**, *125*, 6982 – 6986; b) E. Cabane, T. Keplinger, V. Merk, P. Hass, I. Burgert, *ChemSusChem* **2014**, *7*, 1020 – 1025; c) N. Shida, Y. Koizumi, H. Nishiyama, I. Tomita, S. Inagi, *Angew. Chem. Int. Ed.* **2015**, *54*, 3922 – 3926; *Angew. Chem.* **2015**, *127*, 3994 – 3998; d) F. Zhou, Z. Zheng, B. Yu, W. Liu, W. T. Huck, *J. Am. Chem. Soc.* **2006**, *128*, 16253 – 16258.

[14] B. Li, B. Yu, Q. Ye, F. Zhou, *Acc. Chem. Res.* **2015**, *48*, 229 – 237.

[15] Y. Wu, Y. Huang, H. Ma, *J. Am. Chem. Soc.* **2007**, *129*, 7226 – 7227.

[16] O. Roling, K. De Bruycker, B. Vonhören, L. Stricker, M. Körsgen, H. F. Arlinghaus, B. J. Ravoo, F. E. Du Prez, *Angew. Chem. Int. Ed.* **2015**, *54*, 13126 – 13129; *Angew. Chem.* **2015**, *127*, 13319 – 13323.

[17] a) T. Qian, Y. Li, Y. Wu, B. Zheng, H. Ma, *Macromolecules* **2008**, *41*, 6641 – 6645; b) T. Wu, K. Efimenko, J. Genzer, *J. Am. Chem. Soc.* **2002**, *124*, 9394 – 9395.

[18] a) U. Raviv, S. Giasson, N. Kampf, J.-F. Gohy, R. Jerome, J. Klein, *Nature* **2003**, *425*, 163 – 165; b) Q. Wei, M. Cai, F. Zhou, W. Liu, *Macromolecules* **2013**, *46*, 9368 – 9379.

[19] M. Husemann, D. Mecerreyes, C. J. Hawker, J. L. Hedrick, R. Shah, N. L. Abbott, *Angew. Chem. Int. Ed.* **1999**, *38*, 647 – 649; *Angew. Chem.* **1999**, *111*, 685 – 687.

[20] E. M. Liston, *J. Adhes.* **1989**, *30*, 199 – 218.

[21] X. Wang, H. Hu, Y. Shen, X. Zhou, Z. Zheng, *Adv. Mater.* **2011**, *23*, 3090 – 3094.

[22] D. Dornfeld, S. Min, Y. Takeuchi, *CIRP Ann.* **2006**, *55*, 745 – 768.

[23] R. R. Gattass, E. Mazur, *Nat. Photonics* **2008**, *2*, 219 – 225.

[24] Z. Nie, E. Kumacheva, *Nat. Mater.* **2008**, *7*, 277 – 290.

Received: January 4, 2016
Revised: February 1, 2016